

THE TIME-DEPENDENT DYNAMICAL RESPONSE OF THE THERMOSPHERE TO MAJOR GEOMAGNETIC DISTURBANCES

David Rees

Department of Physics and Astronomy
University College London
Gower Street, London WC1E 6BT, UK

Several recent observations of thermospheric dynamics, made in the polar regions during extremely disturbed geomagnetic periods are reviewed. In general, the magnitude and the variability of winds in the thermospheric polar regions increases with magnetic activity, as measured by any of the conventional indices. However, none of the conventional indices is a particularly good aid to predicting wind magnitudes. In very general terms, two major factors may be considered in describing the wind system. The magnitude of the IMF and, in particular, its southward component, determine the size of the auroral oval, and the strength of the cross-polar cap potential. This determines the size of the auroral oval, the magnitude of the sunward winds in the auroral oval and of those blowing anti-sunward over the polar cap, and is probably the major factor in determining the rate of geomagnetic energy deposition in the thermosphere. Superimposed on this enhanced polar circulation system will be the effects of discrete auroral substorms. From a global view-point, the effect of substorms is to generate a series of strong disturbances which propagate from their source region, usually near magnetic midnight in the auroral oval. The energy associated with discrete substorms is, however, usually a rather small proportion of the total global geomagnetic input during disturbed periods. Some of these substorm-related effects are discussed in more detail in an accompanying paper. A very large asymmetry in the development of polar wind disturbances can be related to the direction and magnitude of the 'Y' component of the IMF. The location of very fast anti-sunward wind jets in the polar cap follows the ion drift asymmetries generated by positive (dusk side maximum) or negative (dawn side maximum) values of the IMF Y component. In the dawn auroral oval and during moderately to very disturbed conditions, strong sunward winds are only observed when the IMF Y component is zero or negative. When the IMF Y component is positive, the winds of the dawn auroral oval are relatively small, or purely equatorward, even during extremely disturbed conditions. These observations of thermospheric wind disturbances will be evaluated by comparison with global simulations of the thermospheric response to theoretical and semi-empirical models of the polar electric field, and of the effects of magnetospheric particle precipitation.

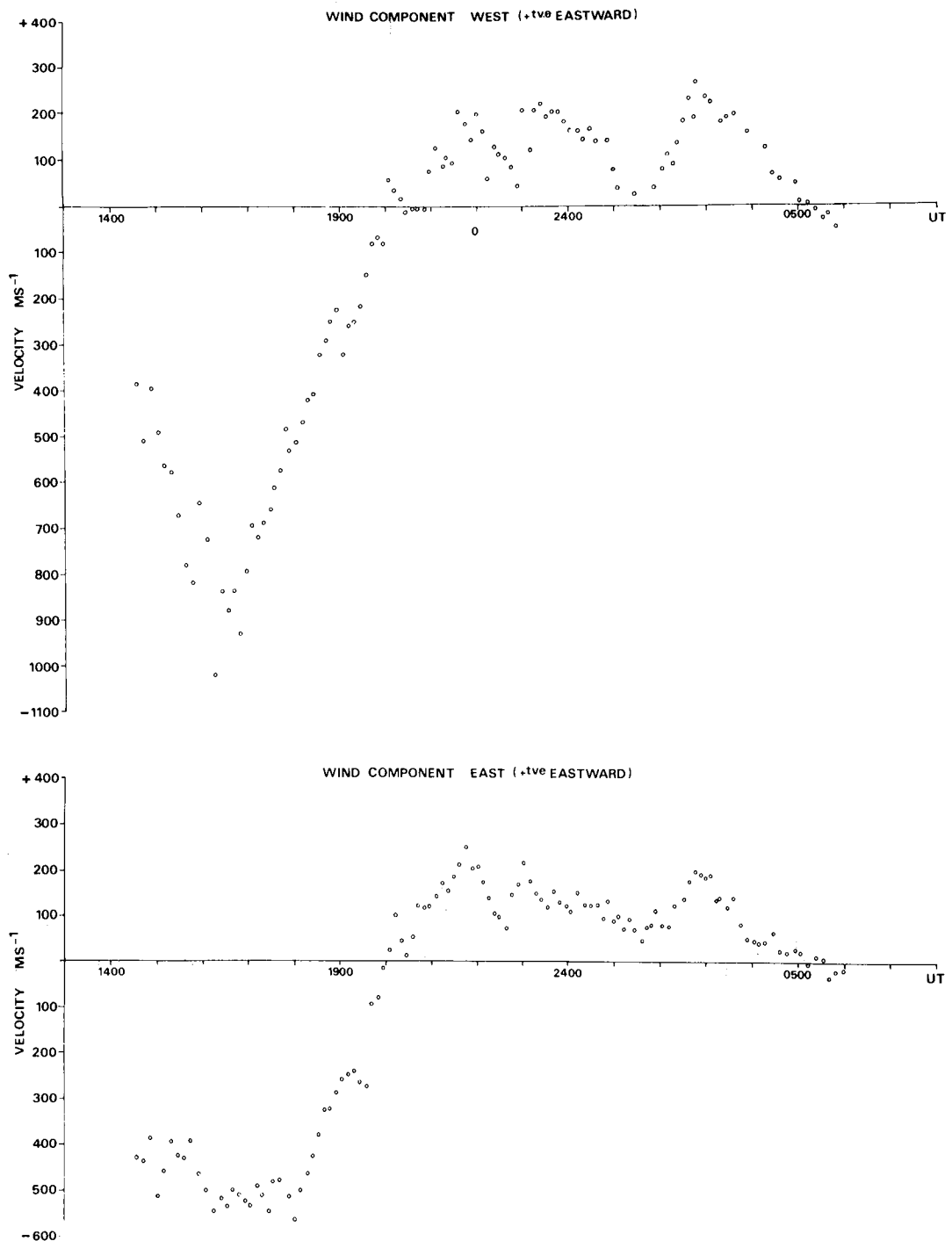
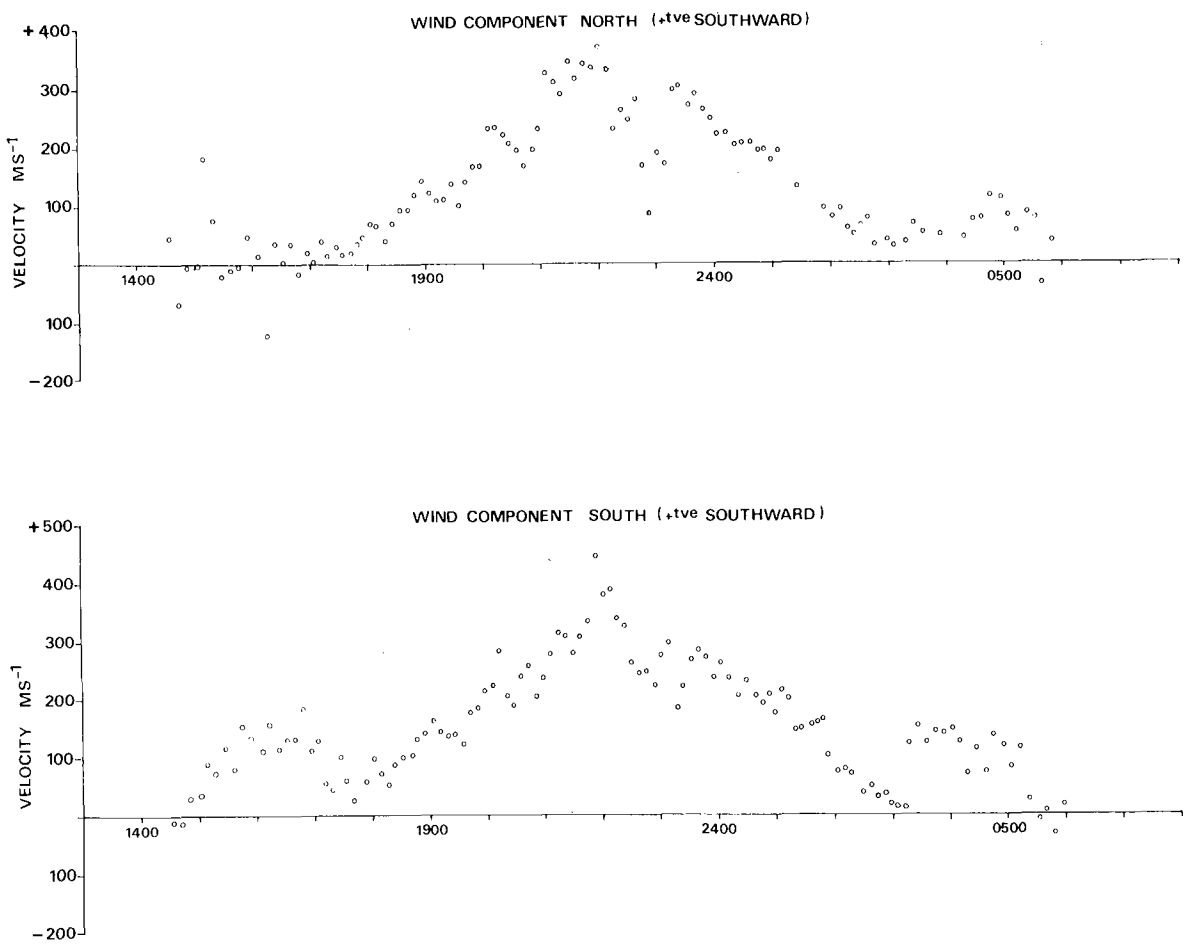


Figure 1. Neutral wind response observed at Kiruna on Dec 12, 1981, by a ground-based fabry-Perot interferometer. Zonal Wind velocity component. Winds are measured in locations 400 km to the east and to the west of Kiruna. Altitude of OI 630 nm emission is about 240 km.



DEC 12/13 1981

Figure 2. As Figure 1, but for the meridional wind component. Meridional components are measured about 400 km to the north and to the south of Kiruna.

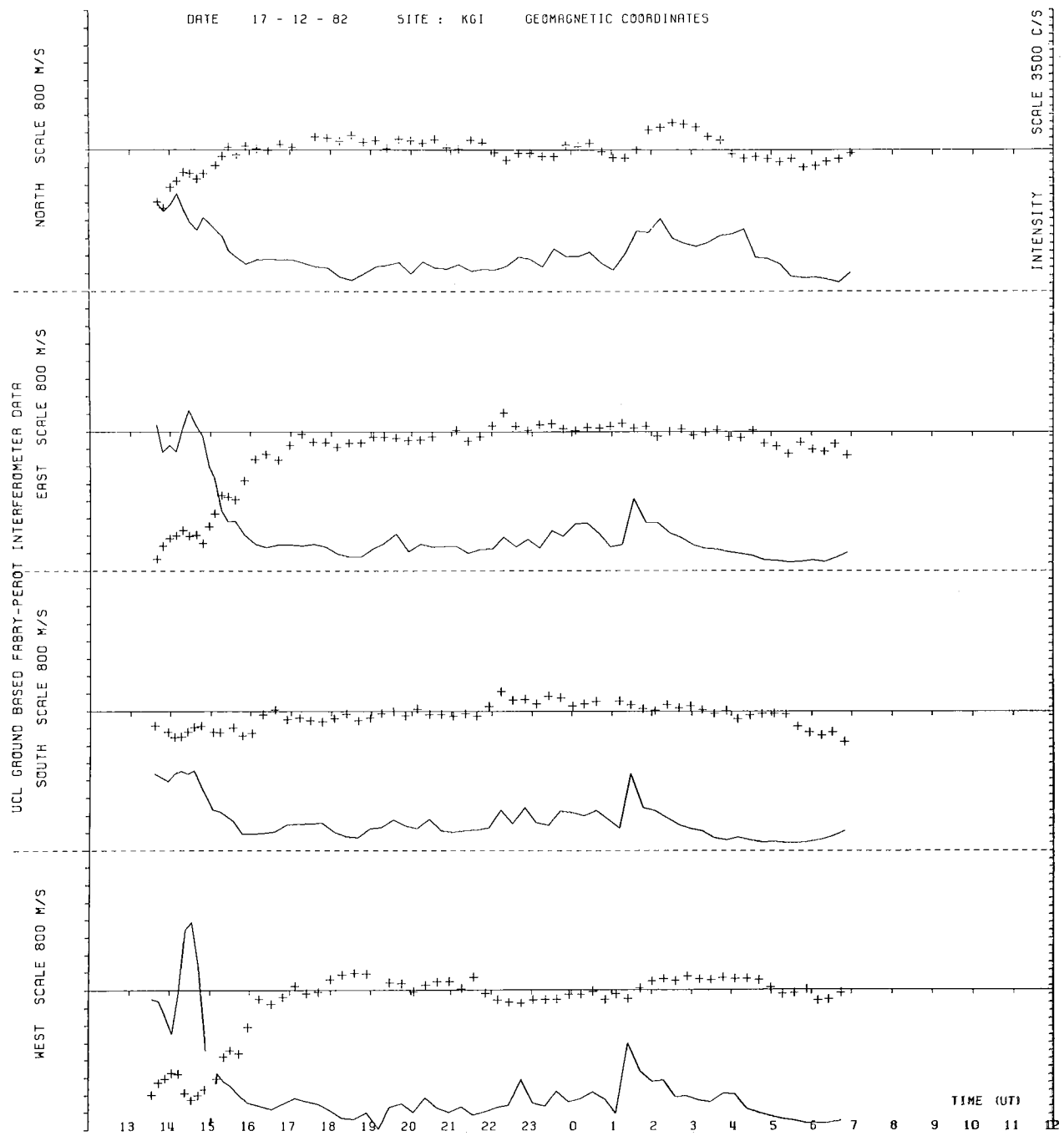


Figure 3. As Figure 1, but for Dec 17, 1982, zonal wind.

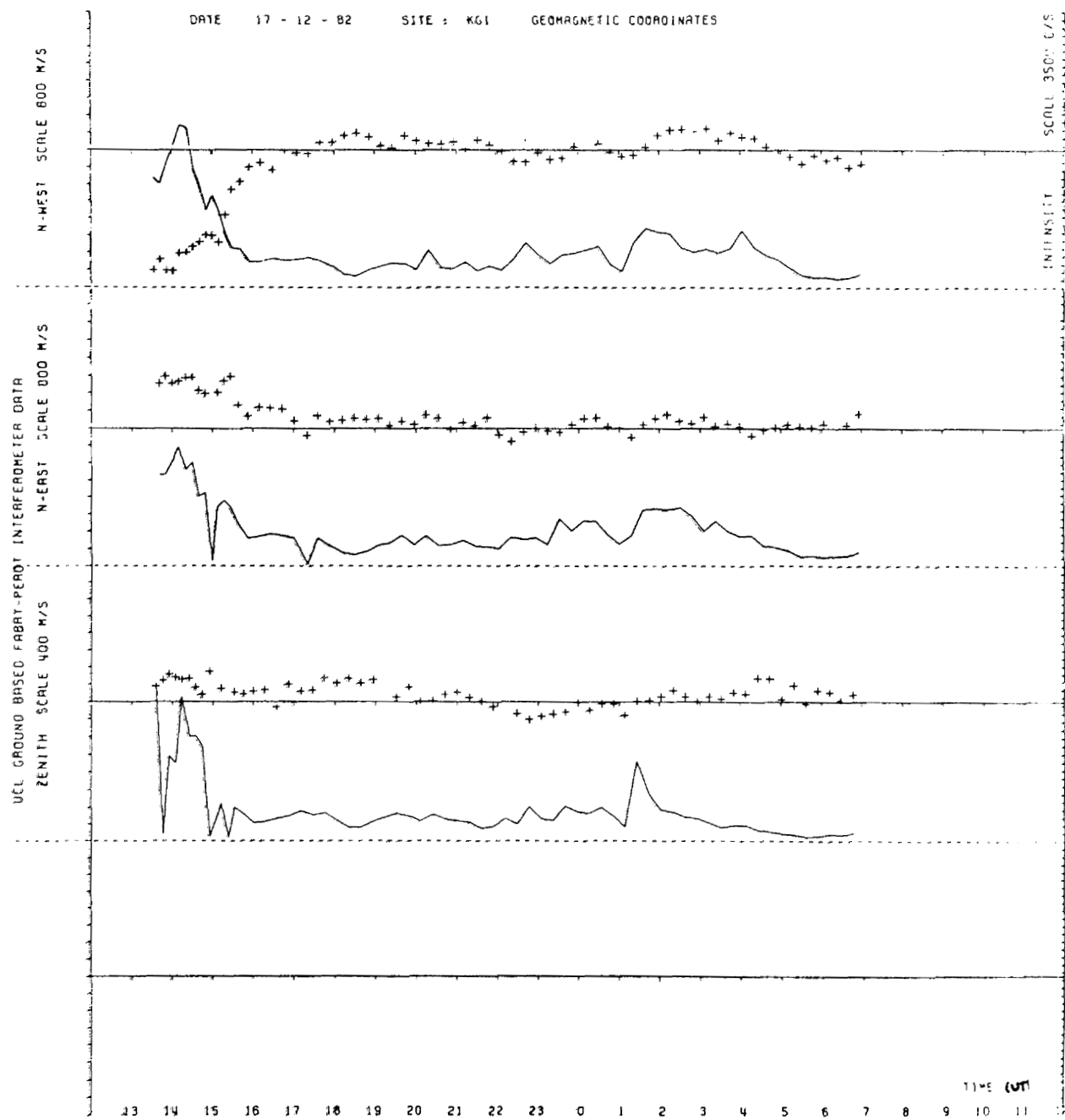


Figure 4. As Figure 3, but for the meridional wind component.

DIRECTION: WEST DATE: 12- 2-82 SITE: K.G.I. SC AGL:45 DG HT: 240 KM

328

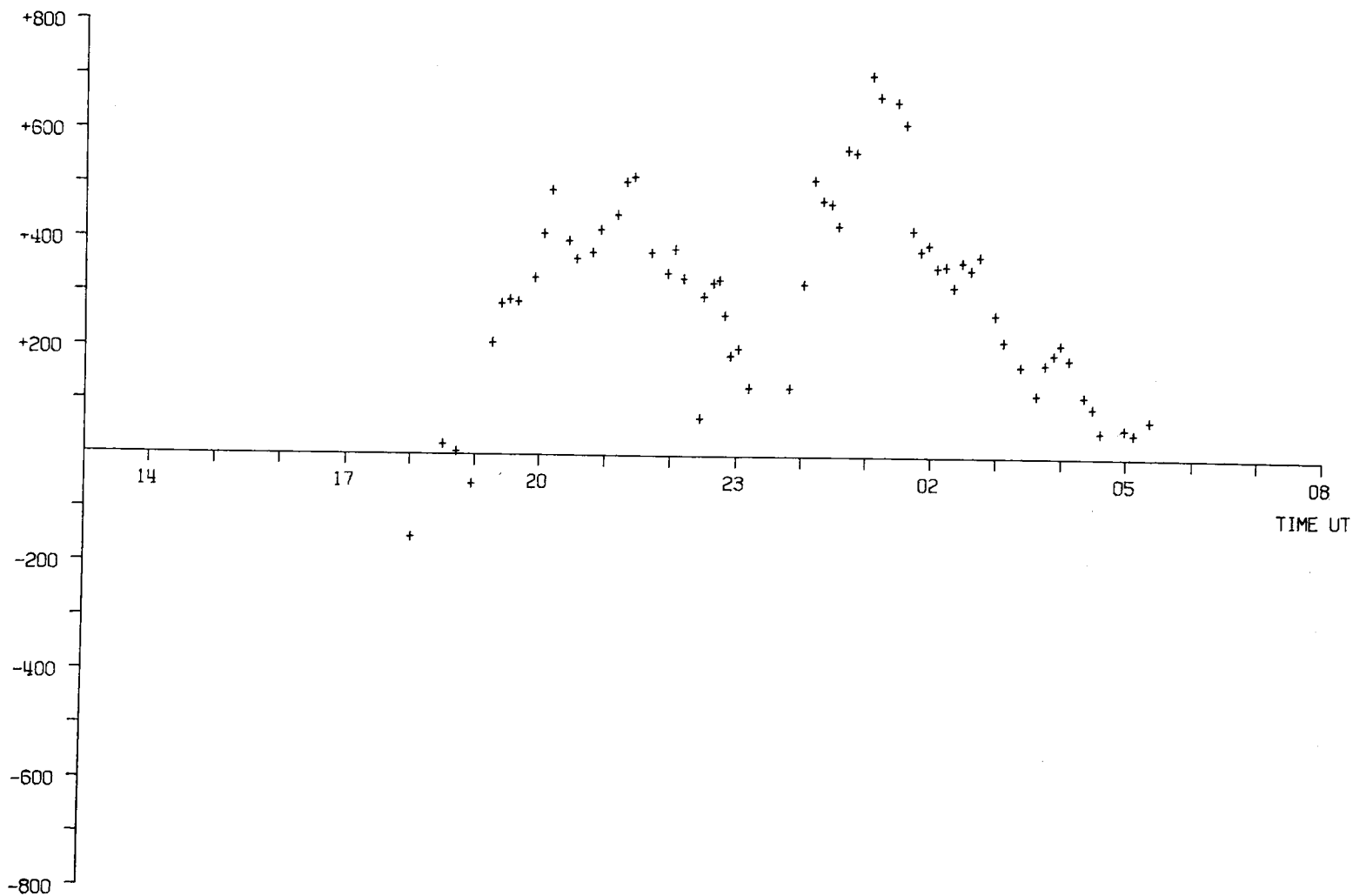


Figure 5. As Figure 1, but for Feb 12/13, 1982, zonal wind.

DIRECTION: NORTH DATE: 12-2-82 SITE: K.G.I. SC AGL: 45 DG HT: 240 KM

329

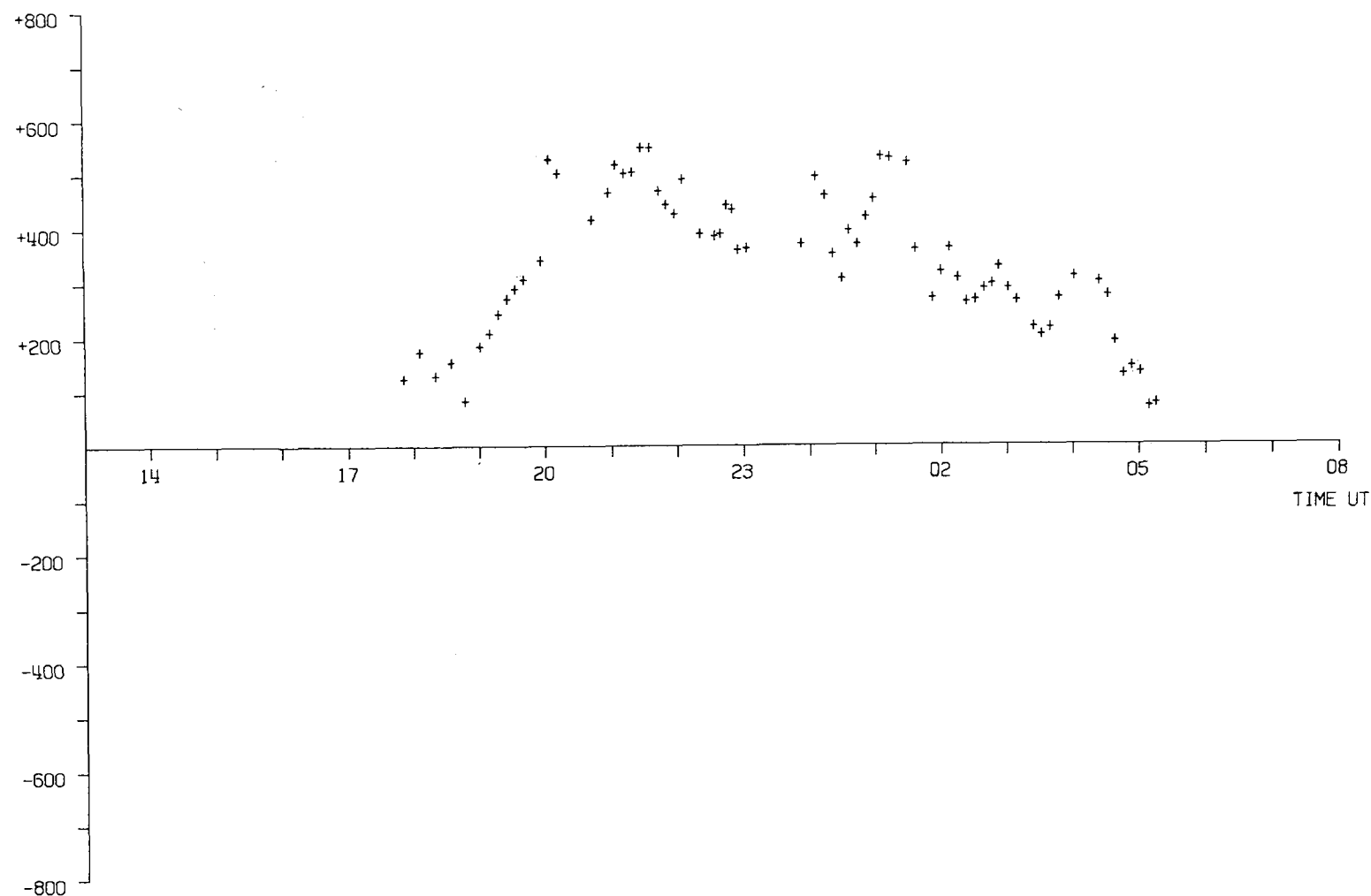


Figure 6. As Figure 5, but for the meridional wind component.

DIRECTION : AEST DATE : 9-10-83 ALT : 1.6.1. SC ANGL : 30.776 HEIGHT : 240 KM

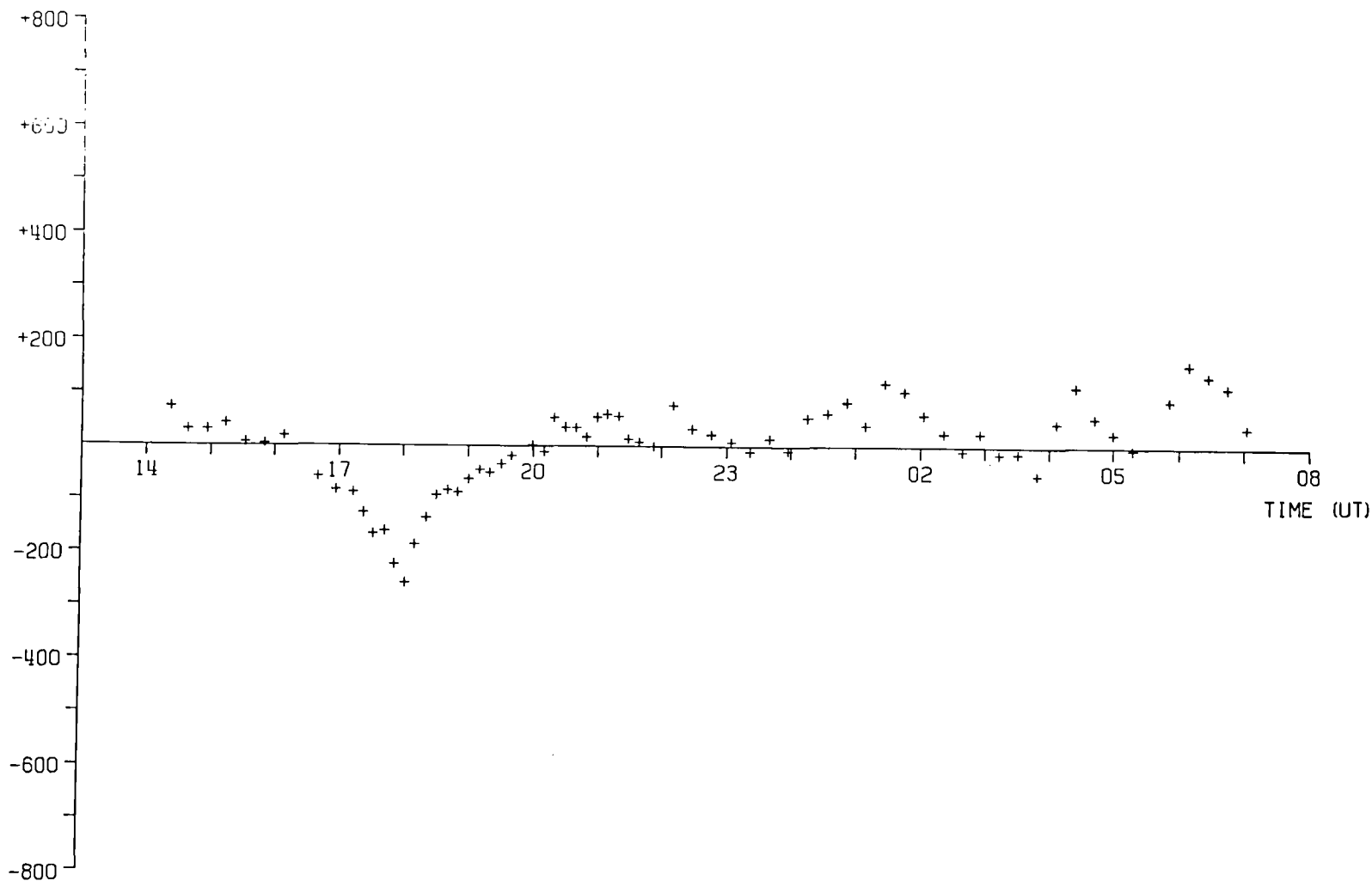


Figure 7. As Figure 1, but for January 9/10 1983, zonal wind.

DIRECTION : NORTH DATE : 9-11-73 SITE : K. I. T. LT ANGL : 30 DEG HEIGHT : 140 KM

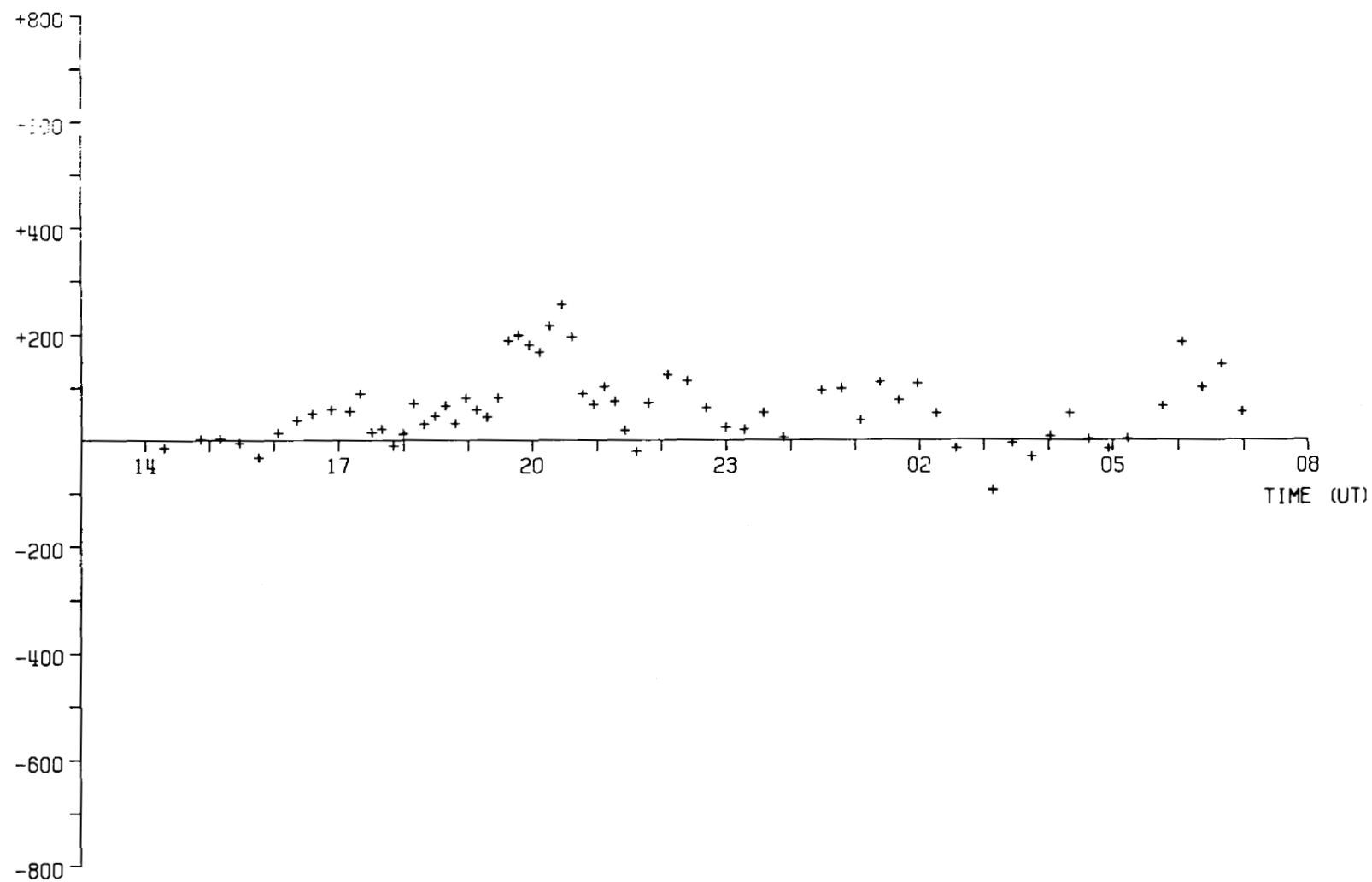
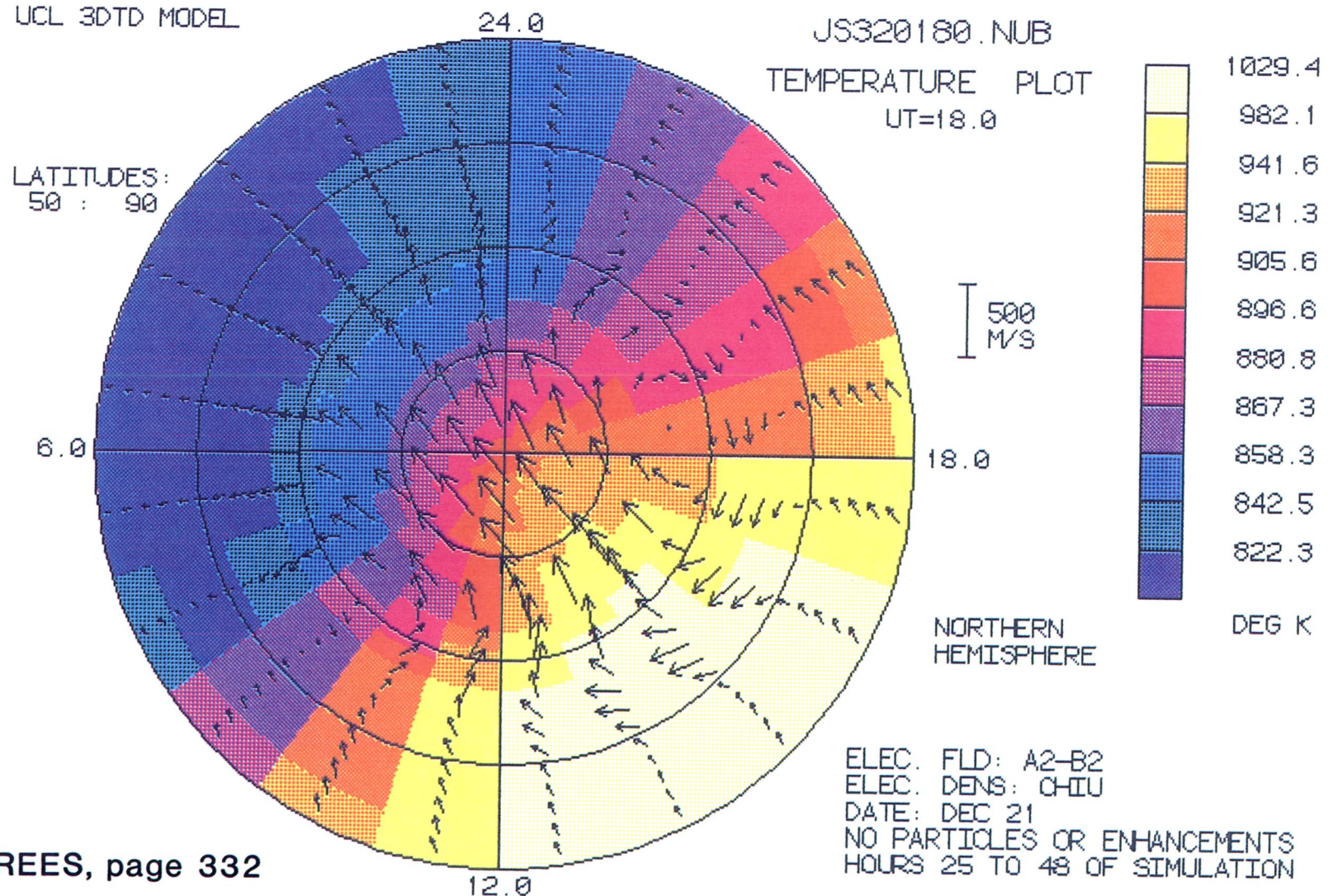


Figure 8. As Figure 7, but for the meridional wind component.

332

UCL 3DTD MODEL

LATITUDES:
50 : 90



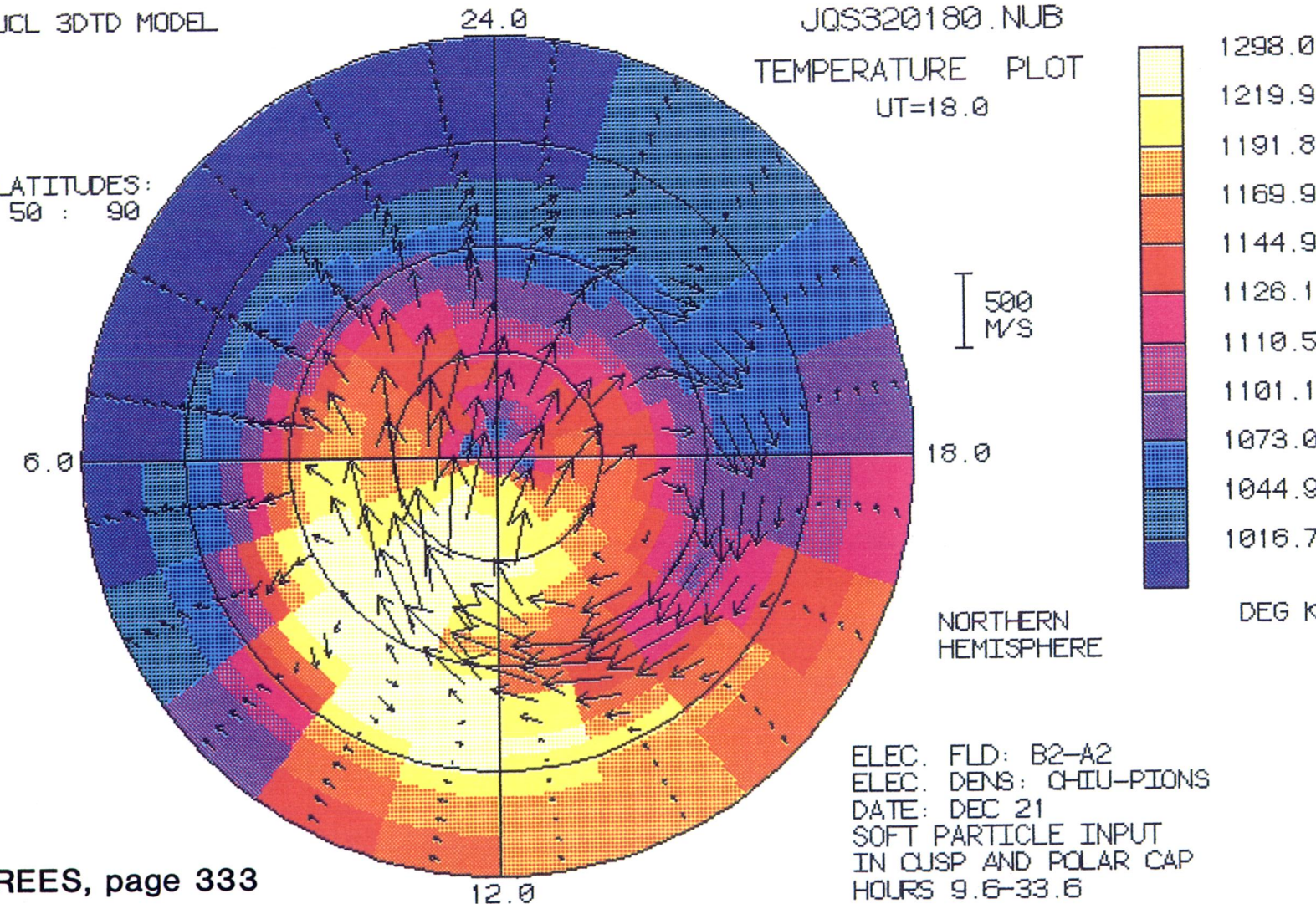
REES, page 332

Figure 9. Thermospheric winds (320 km altitude) from the UCL 3-D T-D model for relatively quiet geomagnetic conditions. (J2 320, 180, NUB, polar)

333

UCL 3DTD MODEL

LATITUDES:
50 : 90



REES, page 333

Figure 10. Thermospheric winds (320 km altitude) from the UCL 3-D T-D model for relatively disturbed geomagnetic conditions. (JQ 320 180, NUB, polar)

334

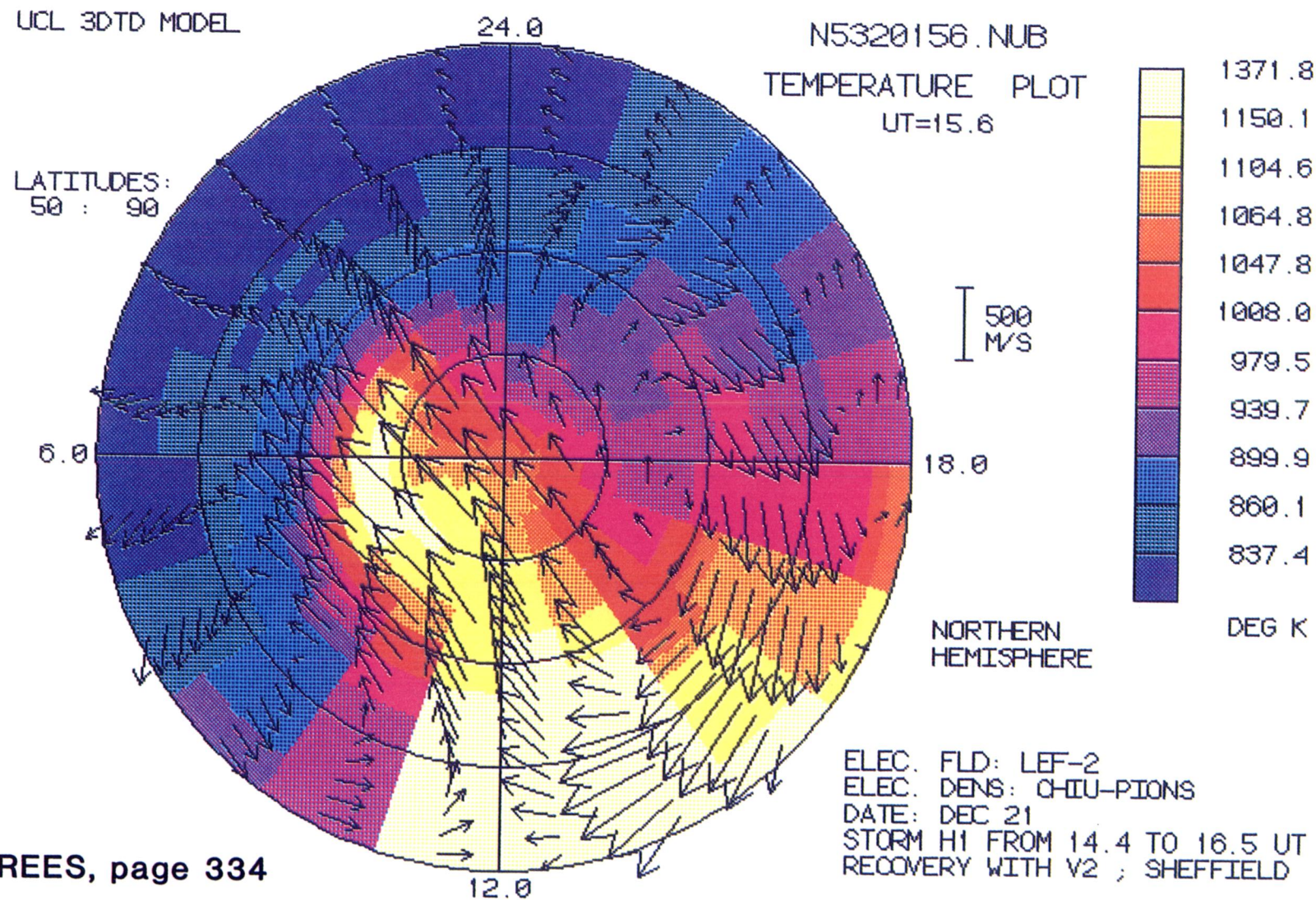
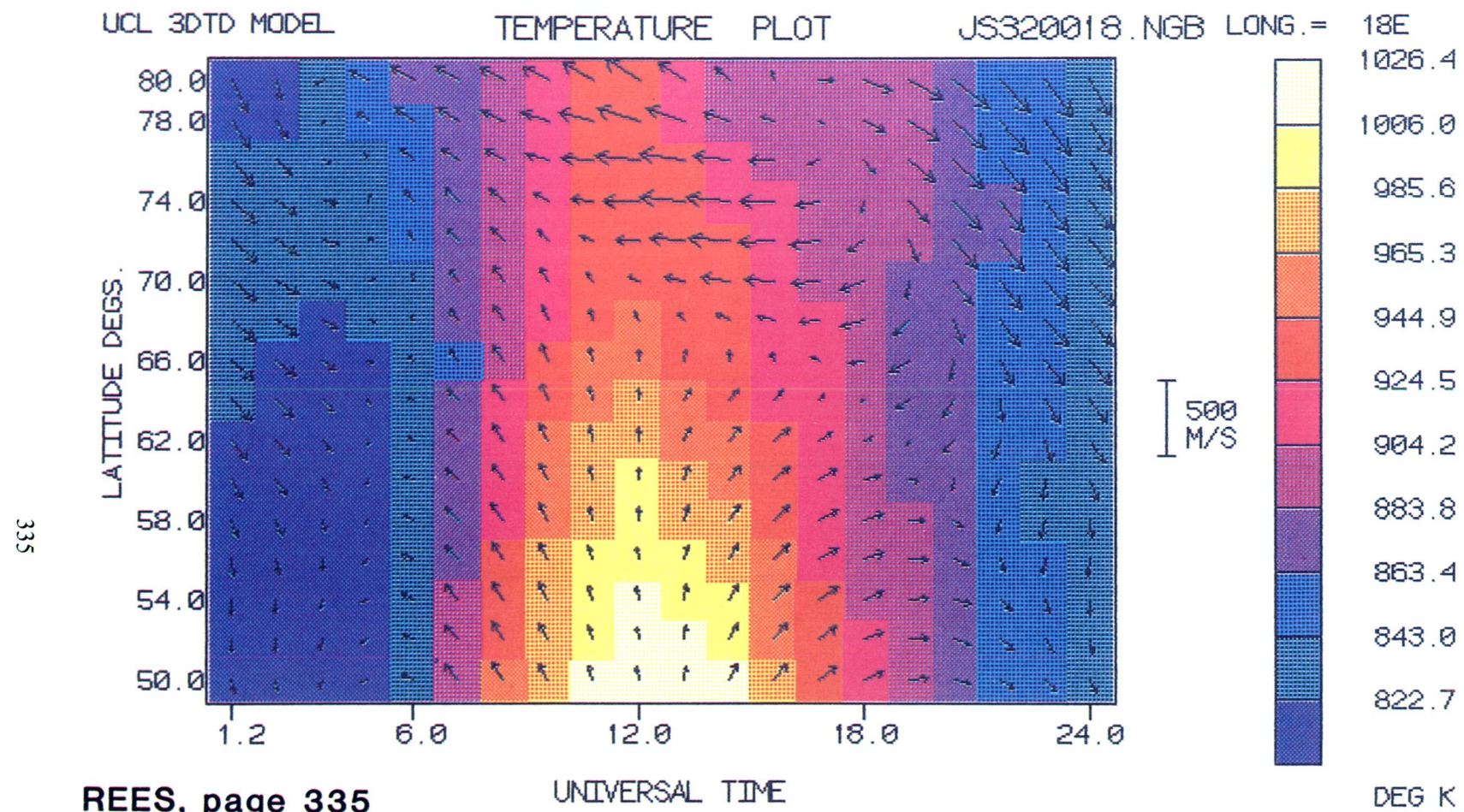


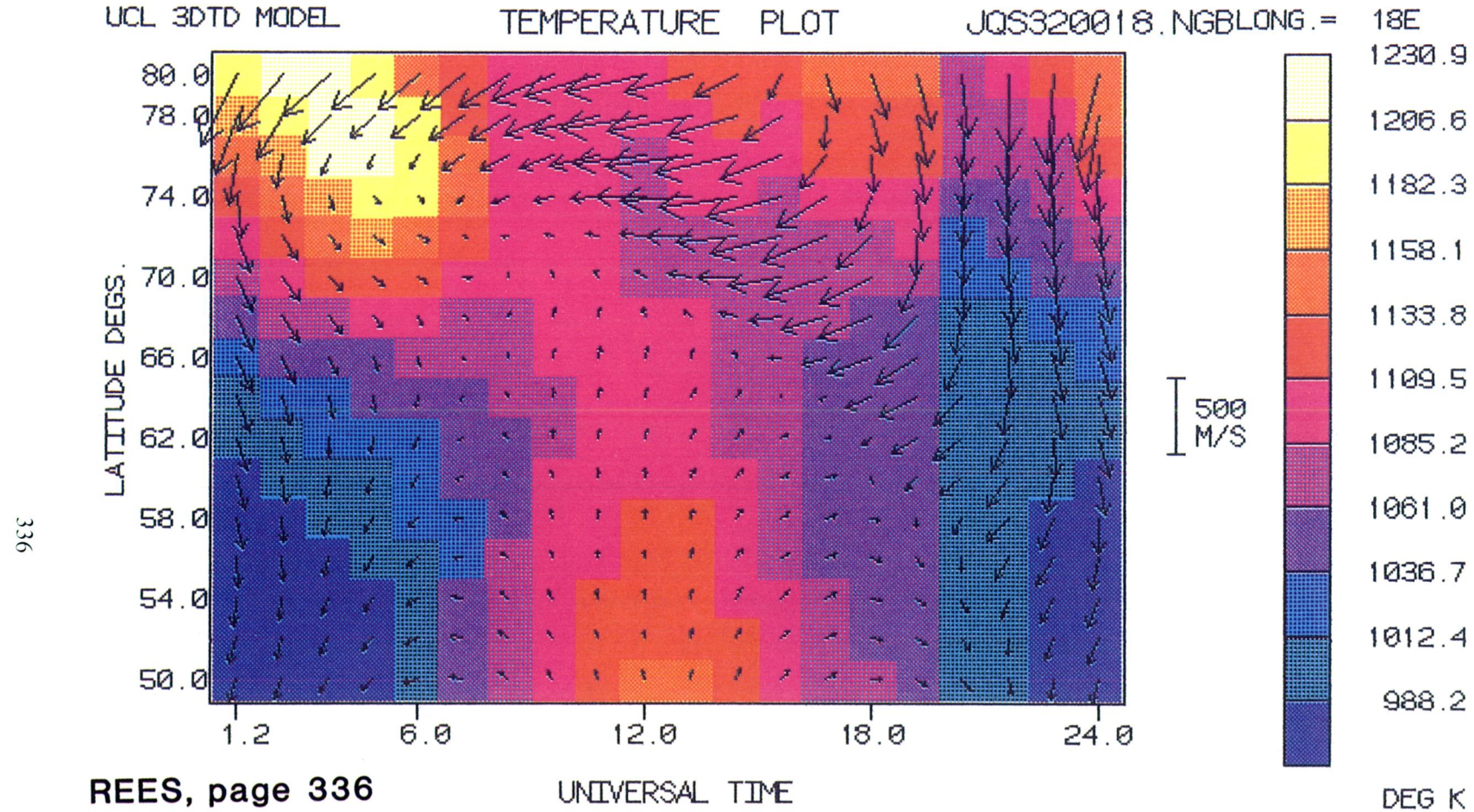
Figure 11. Thermospheric winds (320 km altitude) from the UCL 3-D T-D model for geomagnetic storm conditions. (N4, 320, 156, NUB, polar)



ELEC. FLD: A2-B2
ELEC. DENS: CHIU
DATE: DEC 21

NO PARTICLES OR ENHANCEMENTS
HOURS 25 TO 48 OF SIMULATION

Figure 12. Thermospheric winds (320 km altitude) from the UCL 3-D T-D model for relatively quiet geomagnetic conditions. (J2 320, 018, NGB, CART, 50-80)

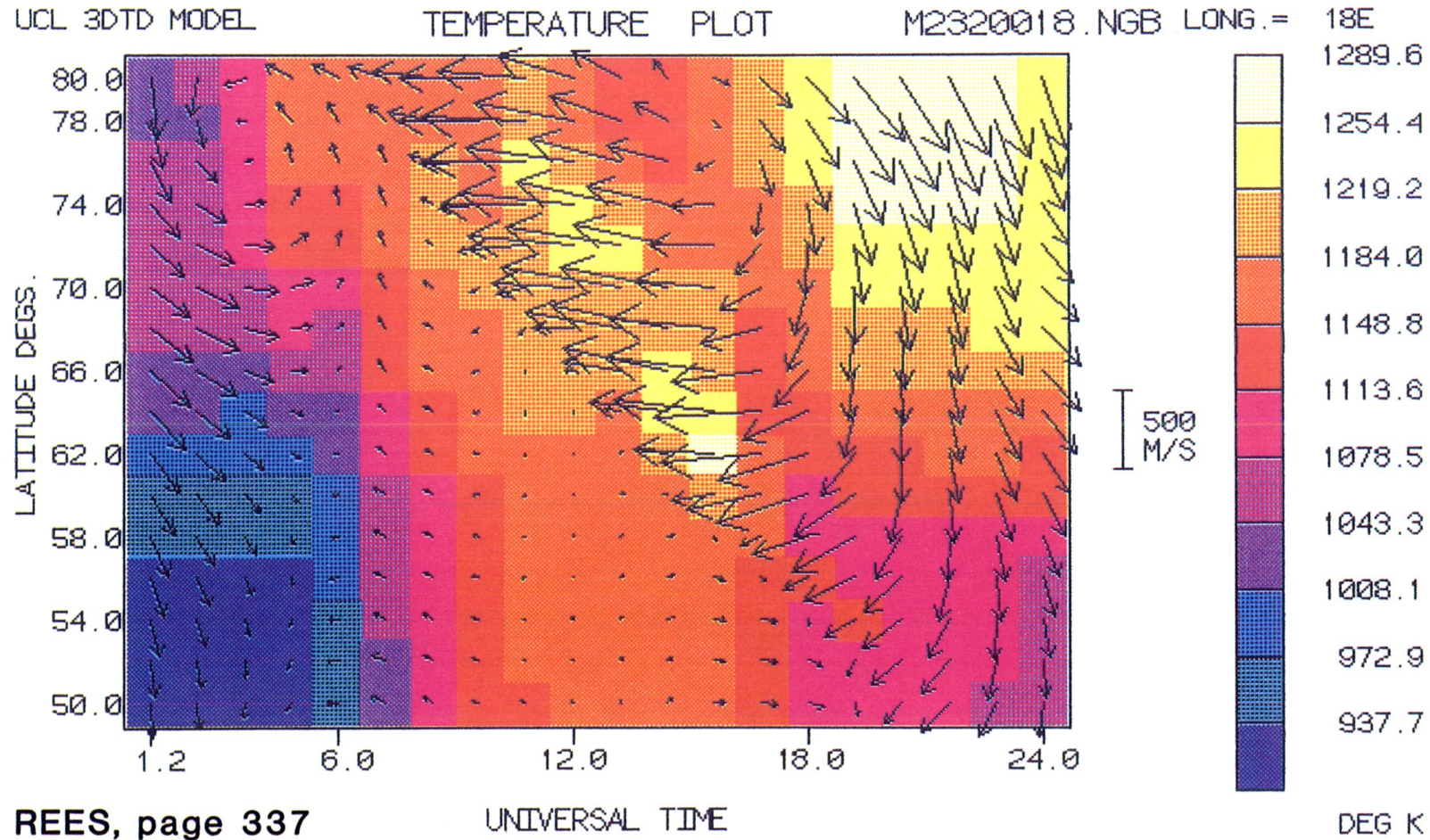


REES, page 336

ELEC. FLD: B2-A2
 ELEC. DENS: CHIU-PIONS
 DATE: DEC 21

SOFT PARTICLE INPUT
 IN CUSP AND POLAR CAP
 HOURS 9.6-33.6

Figure 13. Thermospheric winds (320 km altitude) from the UCL 3-D T-D model for relatively disturbed geomagnetic conditions. (JQ 320, 018, NGB, CART 50-80)



REES, page 337

ELEC. FLD: LEF-1
ELEC. DENS: CHIU
DATE: OCT 16

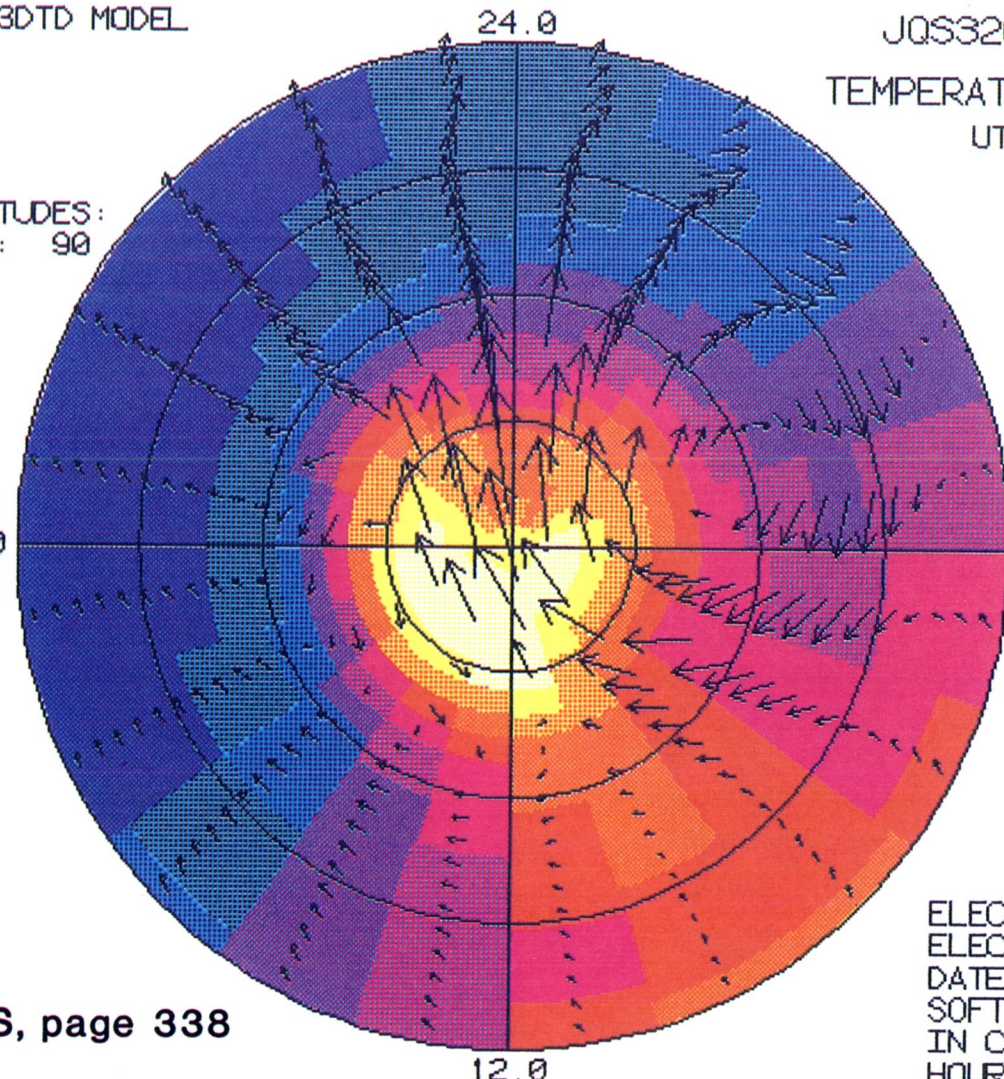
Hrs 25 to 48 of run 2
NO PARTICLES OR ENHANCEMENTS

Figure 14. Thermospheric winds (320 km altitude) from the UCL 3-D T-D model for relatively quiet geomagnetic conditions. (M2 320, 018, NGB, CART, 50-80)

338

UCL 3DTD MODEL

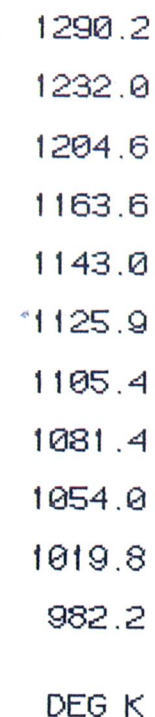
LATITUDES:
50 : 90



JQS320000.NUB
TEMPERATURE PLOT
UT= 0.0

500
M/S

NORTHERN
HEMISPHERE



ELEC. FLD: B2-A2
ELEC. DENS: CHIU-PIONS
DATE: DEC 21
SOFT PARTICLE INPUT
IN CUSP AND POLAR CAP
HOURS 9.6-33.6

REES, page 338

Figure 15. Thermospheric winds (320 km altitude) from the UCL 3-D T-D model for relatively disturbed geomagnetic conditions. (JQ 320, 000 NUB, polar). Simulation for a positive Y component of the IMF.

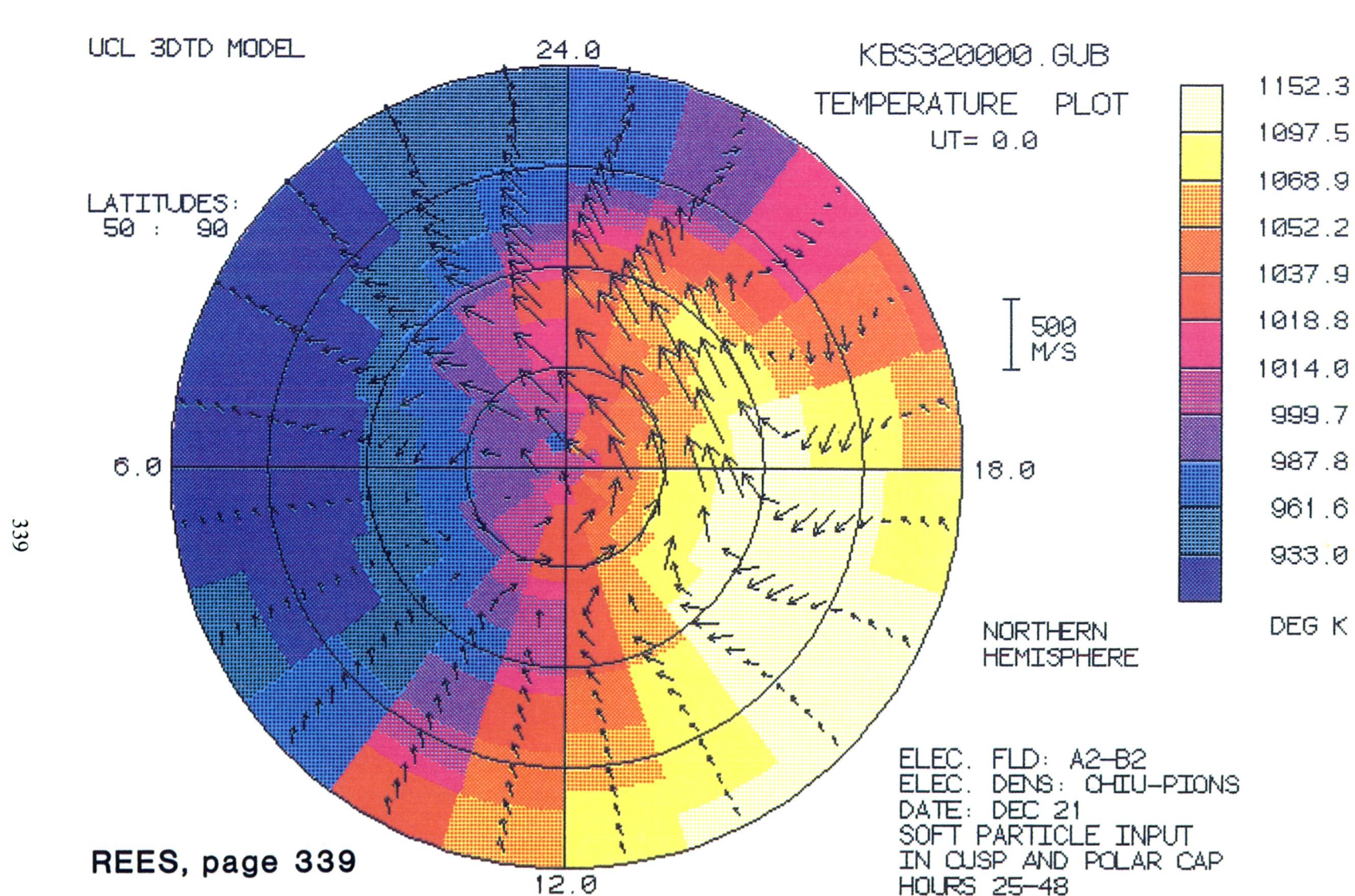


Figure 16. Thermospheric winds (320 km altitude) from the UCL 3-D T-D model for relatively disturbed geomagnetic conditions. (KB2 320, 000, NUB, polar). simulation for a negative Y component of the IMF.